

## INFLUENCE OF SOLVENTS ON SPIN TRANSITION OF [Fe(ABPT)<sub>2</sub>(C(CN)<sub>3</sub>)<sub>2</sub>] SPIN-CROSSOVER MOLECULE

NGUYEN ANH TUAN

*Faculty of Physics, Hanoi University of Science, Vietnam National University, 334  
Nguyen Trai, Thanh Xuan, Hanoi, Vietnam*

**Abstract.** *We present a density-functional study of the influence of solvents on the geometric structure and the electronic structure of the low-spin and high-spin states of [Fe(abpt)<sub>2</sub>(C(CN)<sub>3</sub>)<sub>2</sub>] molecule with abpt = 4-amino-3,5-bis(pyridin-2-yl)-1,2,4-triazole, in order to explore more about the way to control spin-crossover behavior of transition metal molecules. Our calculated results demonstrated that the geometric structure of molecule under consideration is only slightly changed by solvents. However, typical quantities of the electronic structure and spin-transition of this molecule such as the atomic charge, the magnetic moment of Fe ion, the HOMO-LUMO gap, and the spin-state energy difference are varied as a function of dielectric constant of solvents. They reach saturation values with increasing dielectric constant. These results should give some hints to control spin transition temperature of spin-crossover molecules.*

### I. INTRODUCTION

Along with the development of science, technology and human civilization, we are increasingly aware of and issues facing the energy efficiency, fuel, raw materials and natural resources as well as internal about environmental safety... so that we can develop sustainably. In particular the development of the electronics industry challenges associated with "How to compact the size of the components and electronics devices and speed up the process even more"? The challenge now is "How to manufacture the electronic components with size less than 100 nm and speed of response  $\ll 10^{-9}$  s". This challenge requires both a technological breakthrough as well as finding new materials. The finding of molecular magnets has opened a door to go to the world of components and micro-electronic devices because of their size only a few nano-meters. With tiny size and their special physical properties, molecular magnets [1] have opened a new field called molecular spintronics [2,3]. Moreover, with development of nanotechnology, especially the technology of preparing materials and electronic components by using printers [4-8], molecular spintronics becomes a reliable and hot research field. In particular, molecules have spin transition (spin crossover, SCO) may be used to make the switch that the closed and opened states correspond to the low- and high-spin states of the molecule [9]; accompanying the spin transition is the change of color [10], therefore, the SCO molecules can also be applied to the device displays information such as mobile phone screen with an ultra-high resolution; the SCO molecules can also be used to make ultra-high density information storage devices that each molecule is a bit of information, the 0 and 1 states correspond to the low-spin (LS) and high-spin (HS) states of molecules... In the solid state as well

as in solutions, the spin state of SCO molecules can be switched reversibly by an external factor as light, pressure, temperature and magnetic field [9,11].

In this paper, in order to explore more about possibilities of the control of SCO characteristics of SCO molecules, we study influence of solvents on the geometric structure and the electronic structure of the LS and HS states of  $[\text{Fe}^{2+}(\text{abpt})_2(\text{C}(\text{CN})_3)_2]^{-2}$  (hereafter  $[\text{Fe}^{2+}]$ ) with abpt = 4-amino-3,5-bis(pyridin-2-yl)-1,2,4-triazole [12], by employing the conductor-like screening model (COSMO) based on density functional theory (DFT). Our calculated results demonstrated that the dielectric constant of solvents is a key parameter to tailor SCO behavior of  $[\text{Fe}^{2+}]$  molecule. This result should give some hints to control SCO behavior of SCO molecules.

## II. COMPUTATIONAL METHODS

All calculations have been performed by using the DMol<sup>3</sup> code [13] with the double numerical basis sets plus polarization functional. For the exchange correlation terms, the generalized gradient approximation (GGA) PBE functional was used [14]. The effective core potential Dolg-Wedig-Stoll-Preuss was used to describe the interaction between the core and valence electrons [15]. For better accuracy, the hexadecapolar expansion scheme is adopted for resolving the charge density and Coulombic potential. The atomic charge and magnetic moment were obtained by using the Mulliken population analysis [16]. The spin transition state was determined by using the Linear-Synchronous-Transit method [17]. The conductor-like screening model (COSMO) was used to describe the effects of a solvent [18]. The real-space global cutoff radius was set to be 4.6 Å for all atoms. The spin-unrestricted DFT was used to obtain all results presented in this study. The charge density is converged to  $1 \times 10^{-6}$  a.u. in the self-consistent calculation. In the optimization process, the energy, energy gradient, and atomic displacement are converged to  $1 \times 10^{-5}$ ,  $1 \times 10^{-4}$  and  $1 \times 10^{-3}$  a.u., respectively. In order to determine the ground-state atomic structure of the  $[\text{Fe}^{2+}]$  molecule in vacuum as well as in solvents, we carried out total-energy calculations with full geometry optimization, allowing the relaxation of all atoms in this molecule. In addition, to obtain both the geometric structures corresponding to the low-spin and high-spin states of the  $[\text{Fe}^{2+}]$  molecule, both the low-spin and high-spin configurations of the  $\text{Fe}^{2+}$  ion are probed, which are imposed as an initial condition of the structural optimization procedure. In terms of the octahedral field, the  $\text{Fe}^{2+}$  ion could, in principle, has the low-spin state with configuration  $d^6(t_{2g}^6, e_g^0)$  and the high-spin state with configuration  $d^6(t_{2g}^4, e_g^2)$ .

## III. RESULTS AND DISCUSSION

The geometric structure of  $[\text{Fe}^{2+}]$  molecule is depicted in Fig. 1. This molecule has the central symmetry with the symmetric center at the Fe atom. The  $\text{Fe}^{2+}$  ion is located in a distorted octahedron, in which two equivalent bidentate abpt ligands stand in the equatorial plane and two terminal nitrile  $\text{C}(\text{CN})_3$  anions complete the coordination sphere in trans position, as shown in Fig. 1. Due to the central symmetry of the  $[\text{Fe}^{2+}]$  molecule, the N1, N2 and N5 sites are equivalent to the N3, N4 and N6 sites, respectively. Selected bond lengths and bond angles of  $[\text{Fe}^{2+}]$  molecule are tabulated in Table 1. As shown in

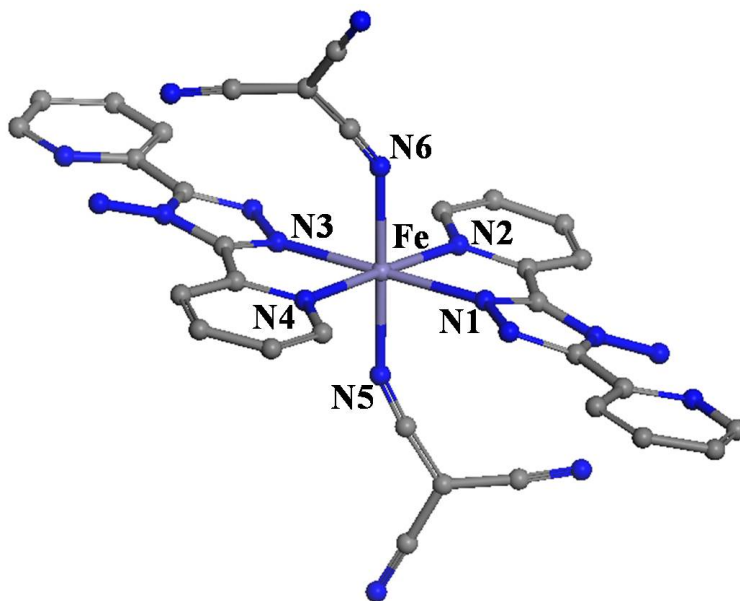


**Fig. 1.** Schematic geometric structure of  $[\text{Fe}^{2+}]$  molecule. H atoms are removed for clarity.

Table 1, there is slight difference in the geometric structure of  $[\text{Fe}^{2+}]$  molecule between the computed results and experimental data reported in reference [12]. Here, it is noted that, calculations have been carried out for the isolated  $[\text{Fe}^{2+}]$  molecule in vacuum. This approximation neglects interactions between neighbouring molecules. Calculations which do not regard these interactions can therefore be different from the experiment.

As shown in Table 1, Fe-N bond lengths of the LS state are always shorter than those of the HS state. This can be explained in terms of ligand field theory. In this  $[\text{Fe}^{2+}]$  molecule, the  $\text{Fe}^{2+}$  ion is located in nearly octahedron forming by six anionic nitrogen ions, as shown in Fig. 1. In terms of octahedral ligand field, the LS state of the  $\text{Fe}^{2+}$  is  $(t_{2g}^6, e_g^0)$  characterized by three fully occupied  $t_{2g}$  orbitals ( $d_{xy}^2, d_{xz}^2, d_{yz}^2$ ) and by two empty  $e_g$  orbitals ( $d_{x^2-y^2}^0, d_{z^2}^0$ ). In the paramagnetic HS state with the electronic configuration  $(t_{2g}^4, e_g^2)$ , five electrons belonging to the majority spin are distributed over all five 3d orbitals according to Hund's rule, the sixth electron that belongs to the minority spin enters a  $t_{2g}$  orbital. It is easy to see that  $e_g$  orbitals are single occupied in the HS state, while they are empty in the LS state. As we know, the electron density in  $e_g$  orbitals is directed toward six anionic nitrogen ions surrounding the  $\text{Fe}^{2+}$  ion, while the electron density in  $t_{2g}$  orbitals is distributed along the bisector of the N-Fe-N angles. Therefore, coulomb repulsion to anion nitrogen ions from  $e_g$  electrons is stronger than that from  $t_{2g}$  electrons. Consequently, the Fe-N bond lengths of the HS state are longer than those of the LS state. As shown in Table 1, the Fe-N bond lengths are typically about 1.95 to 2.02 Å in the LS state, increase by about 10 % upon crossover to the HS state.

**Table 1.** Selected Fe-N bond lengths (in Å) and N-Fe-N bond angles (in degree) of the LS and HS states of the  $[\text{Fe}^{2+}]$  molecule obtained from calculated results and experimental data [12]. Experimental values are shown in italic. The average values of Fe-N bond lengths and N-Fe-N bond angles are shown in bold.

	LS		HS	
Fe-N1	<i>1.996</i>	1.981	<i>2.145</i>	2.172
Fe-N2	<i>2.022</i>	2.008	<i>2.187</i>	2.195
Fe-N3	<i>1.996</i>	1.964	<i>2.145</i>	2.167
Fe-N4	<i>2.022</i>	2.001	<i>2.187</i>	2.194
Fe-N5	<i>1.941</i>	1.902	<i>2.139</i>	2.075
Fe-N6	<i>1.941</i>	1.915	<i>2.139</i>	2.102
	<b>1.986</b>	<b>1.962</b>	<b>2.157</b>	<b>2.151</b>
N1-Fe-N2	<i>80.182</i>	80.549	<i>75.664</i>	75.883
N2-Fe-N3	<i>99.818</i>	99.184	<i>104.336</i>	104.555
N3-Fe-N4	<i>80.182</i>	80.581	<i>75.664</i>	76.316
N1-Fe-N5	<i>91.457</i>	92.903	<i>91.662</i>	85.591
N4-Fe-N5	<i>89.547</i>	88.691	<i>88.960</i>	92.328
N1-Fe-N6	<i>88.543</i>	85.152	<i>88.338</i>	95.003
N4-Fe-N6	<i>90.453</i>	92.596	<i>91.040</i>	86.337
N1-Fe-N4	<i>99.818</i>	99.689	<i>104.336</i>	103.250
N2-Fe-N5	<i>90.453</i>	90.876	<i>91.040</i>	86.549
N3-Fe-N5	<i>88.543</i>	87.436	<i>88.338</i>	94.584
N2-Fe-N6	<i>91.457</i>	87.844	<i>88.960</i>	94.790
N3-Fe-N6	<i>89.547</i>	94.504	<i>91.662</i>	84.812
	<b>90.000</b>	<b>90.000</b>	<b>90.000</b>	<b>90.000</b>

**Table 2.** Selected Fe-N bond lengths (in Å) of the LS and HS states of the  $[\text{Fe}^{2+}]$  molecule in solvents.

Solvent	e	Fe-N1		Fe-N2		Fe-N5	
		LS	HS	LS	HS	LS	HS
Vacuum	1	1.981	2.172	2.008	2.195	1.902	2.075
Bezene	2.284	1.979	2.153	2.013	2.191	1.902	2.095
Chloroform	4.806	1.965	2.159	2.013	2.190	1.896	2.102
Methylene chloride	9.08	1.973	2.151	2.019	2.187	1.899	2.105
Pyridine	12.3	1.966	2.157	2.017	2.189	1.897	2.108
Nitrobenzene	35.7	1.974	2.151	2.020	2.184	1.894	2.113
Dimethyl sulfoxide	46.7	1.969	2.149	2.020	2.188	1.894	2.117
Water	78.54	1.964	2.150	2.026	2.185	1.893	2.115

To explore more about the way to control SCO behavior of the  $[\text{Fe}^{2+}]$  molecule, we have calculated the geometric structure, electronic structure and spin transition of this molecule in seven solvents with difference dielectric constant ( $\epsilon$ ), i.e. Benzene ( $\epsilon = 2.284$ ), Chloroform ( $\epsilon = 4.806$ ), Methylene chloride ( $\epsilon = 9.08$ ), Pyridine ( $\epsilon = 12.3$ ), Nitrobenzene ( $\epsilon = 35.7$ ), Dimethyl Sulfoxide ( $\epsilon = 46.7$ ), and Water ( $\epsilon = 78.54$ ). Our calculated results

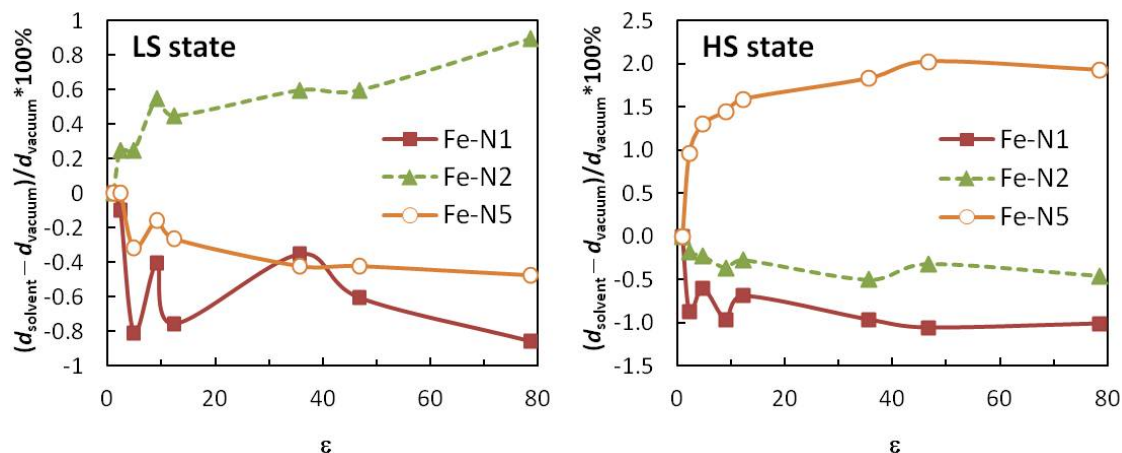


**Fig. 2.** The  $\epsilon$  dependence of the relative difference between the Fe-N bond lengths of  $[\text{Fe}^{2+}]$  molecule in solvents and vacuum.

demonstrate that the geometric structure of the  $[\text{Fe}^{2+}]$  molecule is slightly influent by solvents, as shown in Table 2 and Fig. 2. Fig. 2 shows the  $\epsilon$  dependence of the relative difference between the Fe-N bond lengths of  $[\text{Fe}^{2+}]$  molecule in solvents and vacuum. As described in Fig. 2, the Fe-N bond lengths in the LS state are less influent by solvents than those in the HS state. Each Fe-N bond length tends to reach a constant with the increase of  $\epsilon$ . These results allow us to predict that the electronic structure and SCO behavior also tend to become constant with increasing  $\epsilon$ . To elucidate this, we calculate the atomic charge ( $n$ ), the magnetic moment ( $m$ ), the HOMO-LUMO gap ( $E_{LUMO-HOMO}$ ), and the spin-state energy difference ( $\Delta E$ ).

**Table 3.** The calculated charge [e] of Fe and N1-N6 ions in the LS and HS states of the  $[\text{Fe}^{2+}]$  molecule in vacuum and solvents.

Solvent	e	$n_{Fe}$		$n_{N1}$		$n_{N2}$		$n_{N5}$	
		LS	HS	LS	HS	LS	HS	LS	HS
Vacuum	1	0.387	0.870	-0.245	-0.317	-0.392	-0.448	-0.235	-0.317
Bezene	2.284	0.386	0.873	-0.252	-0.326	-0.398	-0.452	-0.217	-0.314
Chloroform	4.806	0.383	0.880	-0.256	-0.326	-0.402	-0.458	-0.199	-0.313
Methylene chloride	9.08	0.377	0.878	-0.258	-0.331	-0.403	-0.458	-0.192	-0.309
Pyridine	12.3	0.376	0.883	-0.256	-0.330	-0.403	-0.461	-0.190	-0.311
Nitrobenzene	35.7	0.375	0.881	-0.257	-0.332	-0.408	-0.462	-0.188	-0.309
Dimethyl sulfoxide	46.7	0.374	0.881	-0.257	-0.332	-0.406	-0.461	-0.186	-0.309
Water	78.54	0.374	0.881	-0.255	-0.332	-0.408	-0.462	-0.184	-0.309

The calculated charge of Fe and N1-N6 ions in the LS and HS states of the  $[\text{Fe}^{2+}]$  molecule in vacuum and solvents is tabulated in Table 3. Due to the geometric symmetry of the  $[\text{Fe}^{2+}]$  molecule, the charge of the N1, N2 and N5 atoms is similar to the N3, N4 and N6 atoms, respectively. Our calculated results confirm the expectation that the charge of Fe and N1-N6 ions tends to become a constant, as shown in Fig. 3. The charge of Fe ion in the LS state decreases with the increase of  $\epsilon$ , and reaches a constant of 0.374 e. In contrast, the charge of Fe ion in the HS state increases with  $\epsilon$ , and reaches a constant of

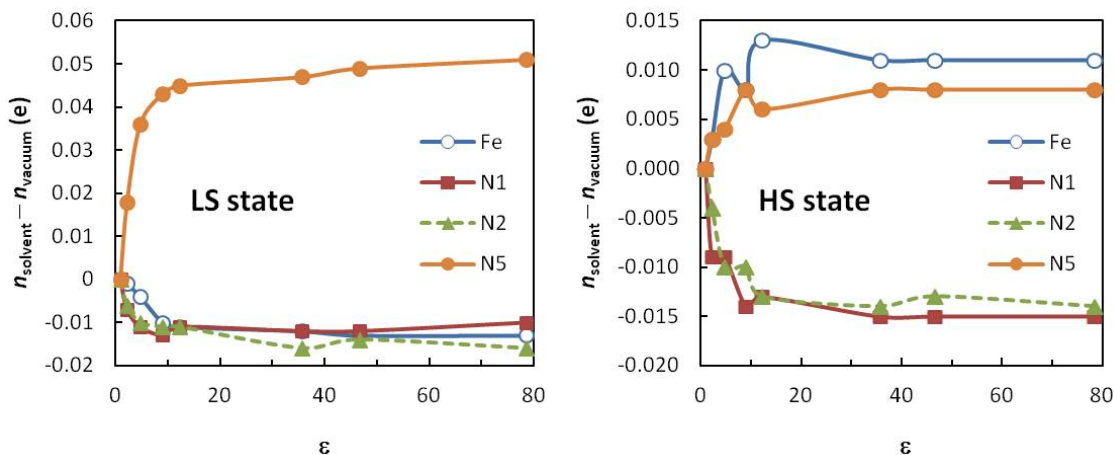


**Fig. 3.** Influence of solvents on the charge of Fe and N1-N6 atoms in the LS and HS states of  $[\text{Fe}^{2+}]$  molecule.

0.881 e. Therefore, the difference in charge of the Fe ion between the LS and HS states increase with  $\epsilon$ , and reaches a constant of 0.507 e, as depicted in Fig. 4.

As shown in Fig. 4 and Table 3, the difference in charge of the Fe ion between the LS and HS states,  $n_{HS-LS}$ , is always positive, while the difference in charge of N ions between the LS and HS states is always negative. These results demonstrate electrons are transferred from the Fe atom to the N atoms by transition from the LS state to the HS state. The charge transfer between the Fe and N atoms increases with  $\epsilon$ , and reaches a saturation value, as shown in Fig. 4. In the water, by transition from the LS state to the HS state of the  $[\text{Fe}^{2+}]$  molecule, amount of charge of 0.507 e is transferred from the Fe atom to the N1-N6 atoms, in which charge transfer to the N1-N6 atoms is 0.077, 0.054, 0.08, 0.055, 0.125, and 0.134 e, respectively.

The  $\epsilon$  dependence of the magnetic moment of Fe atoms ( $m$ ) in the HS state of  $[\text{Fe}^{2+}]$  molecule is depicted in Fig. 5. In vacuum with  $\epsilon = 1$ , the  $m$  is  $3.687 \mu_B$ . The  $m$  increases with increasing  $\epsilon$ , and reaches a saturation value of  $3.700 \mu_B$ . The increase of  $m$  with increasing  $\epsilon$  is consistent with the increase of charge of the Fe atom in the HS state (Fig. 3). Moreover, these results demonstrate that the higher  $\epsilon$ , the more spin down electrons are transferred from the Fe atom to the N1-N6 atoms. Here, it is noted that, the electron configuration of the HS state of  $\text{Fe}^{2+}$  ion is  $(t_{2g}^3 \uparrow, e_g^2 \uparrow, t_{2g}^1 \downarrow)$ . The energy of the spin-down  $t_{2g}^1 \downarrow$  state is higher than those of the spin-up  $t_{2g}^3 \uparrow$  and  $e_g^2 \uparrow$  states. Therefore, charge transfer from the Fe atom to the N1-N6 atoms must come from the  $t_{2g}^1 \downarrow$  state of the Fe atom.

The  $\epsilon$  dependence of the HOMO-LUMO gap ( $E_{LUMO-HOMO}$ ) of the LS and HS states of  $[\text{Fe}^{2+}]$  molecule is displayed in Fig. 6. Our calculated results show that the HOMO-LUMO gaps of the LS and HS states of  $[\text{Fe}^{2+}]$  molecule increase with increasing  $\epsilon$ , and reach saturation values of about 1.625 eV and 0.731 eV, respectively. The increase of the HOMO-LUMO gap of the  $[\text{Fe}^{2+}]$  molecule with increasing  $\epsilon$  allows us to predict

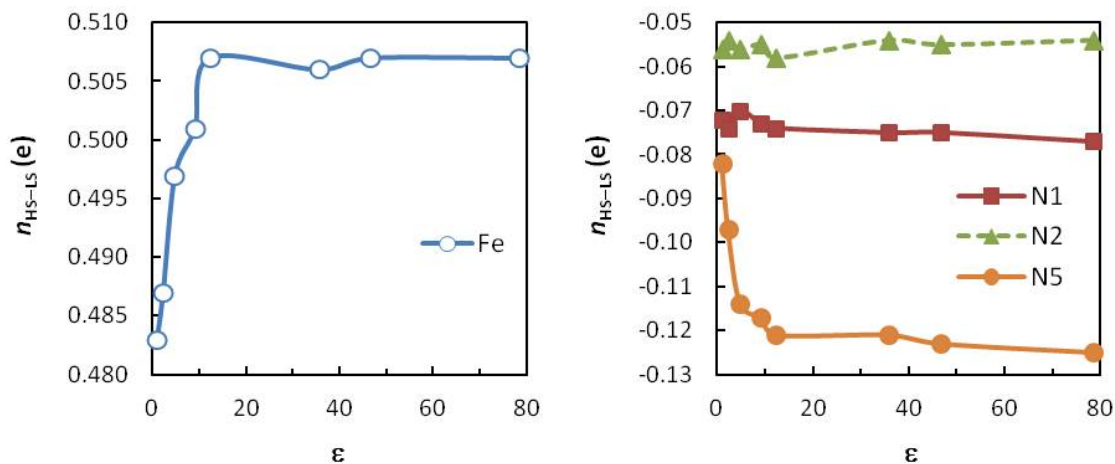


**Fig. 4.** Influence of solvents on the charge transfer upon crossover from the LS state to the HS state of  $[\text{Fe}^{2+}]$  molecule.

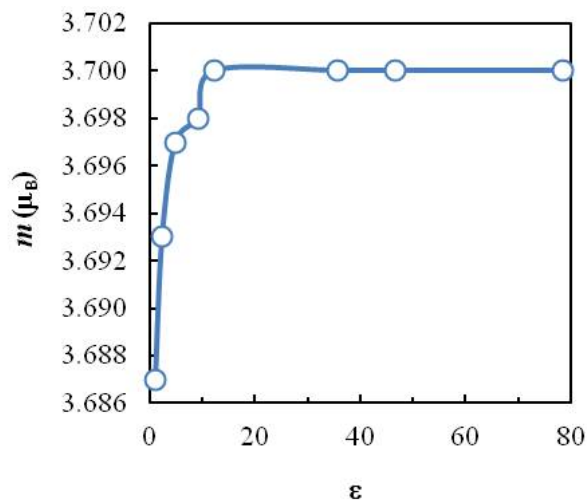


**Fig. 5.** The  $\varepsilon$  dependence of the magnetic moment of Fe atom in the HS state of  $[\text{Fe}^{2+}]$  molecule.

that  $[\text{Fe}^{2+}]$  molecule becomes more stable in solvents with higher  $\varepsilon$ . To shed light on this expectation, we compute the binding energy of  $[\text{Fe}^{2+}]$  molecule ( $E_b$ ). Our calculated results show that the  $E_b$  become more negative with increasing  $\varepsilon$ , as illustrated in Fig. 7. In addition, the  $E_b$  of LS state is larger than that of the HS state. This is consistent with the fact that the LS state is more stable than the HS state.

The difference in the  $E_b$  between the LS and HS states is equal to the spin-state energy difference  $\Delta E$  (the total electronic energy difference between the LS and HS states). By this remark, it is easy to obtain  $\Delta E$ . Our calculated results show that  $\Delta E$  increases

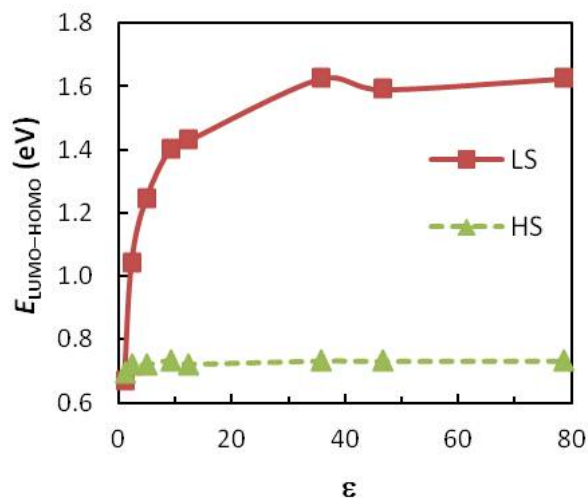


**Fig. 6.** The  $\epsilon$  dependence of the HOMO-LUMO gap of the LS and HS states of  $[\text{Fe}^{2+}]$  molecule.

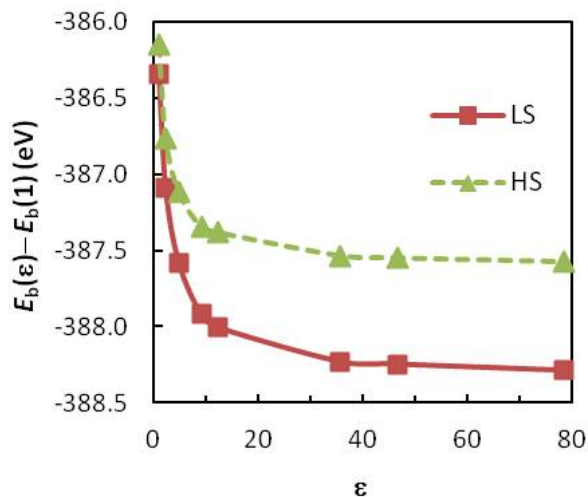


**Fig. 7.** Influence of solvents on the binding energy ( $E_b$ ) of the LS and HS states of  $[\text{Fe}^{2+}]$  molecule.

with increasing  $\epsilon$ , and reach a saturation value of 0.710 eV, as shown in Fig. 8. This behavior is also observed for other SCO complexes [19,20]. Moreover,  $\Delta E$  is proportional to the SCO temperature of  $[\text{Fe}^{2+}]$  molecule ( $t_{\text{SCO}}$ ) [21,22]. These results allow us to predict that the SCO temperature of  $[\text{Fe}^{2+}]$  molecule ( $t_{\text{SCO}}$ ) also increase with increasing  $\epsilon$ .



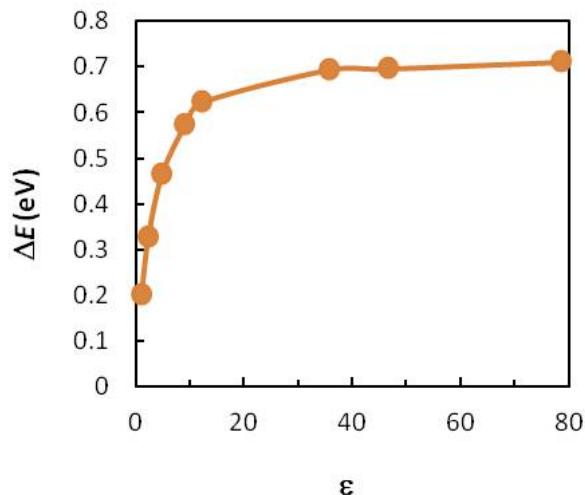


**Fig. 8.** The  $\epsilon$  dependence of the spinstate energy difference ( $\Delta E = E_{HS} - E_{LS}$ ) of  $[\text{Fe}^{2+}]$  molecule.

#### IV. CONCLUSION

The influence of solvents on the geometric structure and electronic structure of the LS and HS states of the  $[\text{Fe}^{2+}]$  molecule has been investigated based on DFT, in order to explore more about the way to control spin crossover behavior of transition metal molecules. Our calculated results demonstrated that the geometric structure of molecule under consideration is slightly changed by solvents. Typical quantities of the electronic structure and spin transition of this molecule such as the atomic charge, the magnetic moment of Fe ion, the HOMO-LUMO gap, and the spinstate energy difference are varied as a function of dielectric constant of solvents. They reach saturation values with increasing dielectric constant. The transition from the LS state to the HS state is accompanied with electron transfer from the  $t_{2g}^1$  state of the Fe atom to surrounding N atoms. This charge transfer also increases with increasing the dielectric constant of solvents. Our calculated results demonstrated that the dielectric constant of solvents is a key parameter to tailor SCO behavior of  $[\text{Fe}^{2+}]$  molecule. These results should give some hints to control SCO behavior of spin crossover molecules.

#### ACKNOWLEDGMENT

We thank Vietnam National University (Hanoi) for funding this work within project QG-11-05 and QGTD-09-05. The computations presented in this study were performed at the Information Science Center of Japan Advanced Institute of Science and Technology, and the Center for Computational Science of the Faculty of Physics, Hanoi University of Science, Vietnam

#### REFERENCES

- [1] Bernd Pilawa, *Ann. Phys.* **8** (1999) 191-254.

- [2] Alexandre R. Rocha, Víctor M. García-suárez, Steve W. Bailey, Colin J. Lambert, Jaime Ferrer, Stefano Sanvito, *Nature Materials* **4** (2005) 335-339.
- [3] Stefano Sanvito, *Chem. Soc. Rev.* **40** (2011) 3336-3355.
- [4] T. Shimoda, Y. Matsuki, M. Furusawa, T. Aoki, I. Yudasaka, H. Tanaka, H. Iwasawa, D. Wang, M. Miyasaka, Y. Takeuchi, *Nature* **440** (2006) 783.
- [5] Y. Y. Noh, N. Zhao, M. Caironi, H., *Nature Nanotechnol.* **2** (2007) 784-789.
- [6] J. Rivnay *et al.*, *Nature Mater.* **8** (2009) 952-958.
- [7] H. Yan, *Nature* **457** (2009) 679-686.
- [8] H. Minemawari, T. Yamada, H. Matsui, J. Tsutsumi, S. Haas, R. Chiba, R. Kumai, T. Hasegawa, *Nature* **475** (2011) 364-367.
- [9] Azzedine Bousseksou, Gábor Molnár, Galina Matouzenko, *Eur. J. Inorg. Chem.* (2004) 4353-4369.
- [10] Gloria Agustí, Ana Belén Gaspar, M. Carmen Munoz, Jse Antonio Real, *Inorg. Chem.* **46** (2007) 9646-9654.
- [11] Philipp Gtlich, Harold A. Goodwin, *Top Curr Chem* **233** (2004) 1-47.
- [12] Gaelle Dupouy, Mathieu Marchivie, Smail Triki, Jean SalaPala, JeanYves Salan, Carlos J. GómezGarcía, Philippe Guionneau, *Inorg. Chem.* **47** (2008) 8921-8931.
- [13] B. Delley, *J. Chem. Phys.* **92** (1990) 508.
- [14] J. P. Perdew, K. Burke, M. Ernzerhof, *Phys. Rev. Lett.* **77** (1996) 3865.
- [15] M. Dolg, U. Wedig, H. Stoll, H. Preuss, *J. Chem. Phys.* **86** (1987) 866; A. Bergner, M. Dolg, W. Kuechle, H. Stoll, H. Preuss, *Mol. Phys.* **80** (1993) 1431.
- [16] R. S. Mulliken, *J. Chem. Phys.* **23** (1955) 1833; R. S. Mulliken, *J. Chem. Phys.* **23** (1955) 1841.
- [17] T. A. Halgren, W. N. Lipscomb, *Chem. Phys. Lett.* **49** (1977) 225.
- [18] A. Klamt, G. Schüürmann, "COSMO: A new approach to dielectric screening in solvents with explicit expressions for the screening energy and its gradient", *J. Chem. Soc.* **2** (1993) 79; B. Delley, "The conductorlike screening model for polymers and surfaces", *Mol. Simul.* **32** (2006) 117-123.
- [19] H. Paulsen, A. X. Trautwein, *J. Phys. Chem. Sol.* **65** (2004) 793-798.
- [20] J. W. Turner, F. A. Schultz, *Inorg. Chem.* **40** (2001) 5296.
- [21] P. Gütllich, H. Köppen, R. Link, H. G. Steinhäuser, *J. Chem. Phys.* **70** (1979) 3977.
- [22] H. Paulsen; J. A. Wolny, A. X. Trautwein, *Monatshefte fr Chemie* **136** (2005) 1107-1118.

*Received 30-09-2011.*